(27) Beever, W. H.; Stille, J. K. *J. Polym. Sci., Polym. Symp.* **1978**, *No. 65*, 41.
(28) Van der Kerk, G. J. M.; Noltes, J. G.; Luijten, J. G. A. *J. Appl. Chem.* **1957**, *7*, 366.
(29) Still, W. C.; Kahn, M.; Mitra, A. *J. Org. Chem.* **1978**, *43*, 2923.
(30) Gordon, A. J.; Ford, R. A. "The Chemist's Companion"; Wiley: New York, 1972; p 180.
(31) Sloan, G. J.; Vaughan, W. R. *J. Org. Chem.* **1957**, *22*, 750.
(32) Perrin, D. D.; Armarego, W. L. F.; Perrin, D. R. "Purification of Laboratory Chemicals", 2nd ed.; Pergamon Press: New York, 1980; p 141.
(33) Ning, R. Y.; Madan, P. B.; Sternbach, L. H. *J. Heterocycl. Chem.* **1974**, *11*, 107.
(34) Davis, R. B.; Pizzini, L. C. *J. Org. Chem.* **1960**, *25*, 1884.
(35) Hetzheim, A.; Haack, H.; Beyer, H. *Z. Chem.* **1966**, *6*, 218.
(36) Coulson, D. R. *Inorg. Synth.* **1972**, *13*, 121.

Polymerization Properties of Amphiphilic Diacetylene Pyridinium and Bipyridinium Salts in the Crystalline State, in Multilayers, and in Aqueous Dispersions

Bernd Tieke*† and Günter Lieser‡

Institut für Makromolekulare Chemie der Universität, Hermann-Staudinger-Haus, D-7800 Freiburg i.Br., West Germany. *Received May 8, 1984*

ABSTRACT: Surface-active *N*-alkylpyridinium salts and *N,N'*-dialkyl-4,4'-bipyridinium salts were synthesized carrying long aliphatic chains with a diacetylene unit in the midchain position. All compounds polymerized in the solid state, when exposed to UV and γ-irradiation. In the case of the *N*-alkylpyridinium salts a complete conversion to polymer was obtained. X-ray structure studies revealed a head–head–tail–tail arrangement of the amphiphiles. During polymerization the structure was completely retained. Some of the *N*-alkylpyridinium salts formed polymers, which were soluble in a 1:1 mixture of chloroform and methanol. Monomeric crystals of the bipyridinium salts showed solid-to-solid and solid-to-liquid crystalline phase transitions, which disappeared upon the polymerization process. Monolayers of the amphiphiles at the air–water interface were of low stability and could be transferred onto substrates only in mixtures with cadmium arachidate. UV irradiation of the mixed multilayers caused a solid-state polymerization of the diacetylene amphiphiles on the substrate. Aqueous suspensions of the monomeric *N*-alkylpyridinium salts turned into clear, micellar solutions at temperatures above 46.5 °C. Sonication of aqueous dispersions resulted in the formation of translucent, slightly opaque solutions in which the amphiphiles formed spherical aggregates of diameters between 100 and 250 nm. Micellar solutions as well as dispersions of the spherical aggregates were completely photoinactive in UV light. However, the spherical aggregates rapidly rearranged into thin particles of oval or polygonal shape of more than 1 μm in diameter (multilamellar layers), which were highly photoreactive. The polymerized amphiphile dispersions neither disintegrated into micelles at elevated temperature nor precipitated within several weeks.

Introduction

In recent years it has been demonstrated that the UV-initiated solid-state polymerization of diacetylene derivatives[1,2] can also be applied to lipid bilayer-type structures. Amphiphilic molecules with diyne units in the aliphatic chains are photoreactive in monomolecular layers, Langmuir–Blodgett (LB) type multilayers, and liposomes,[3-8] provided that the molecules form a condensed phase with a crystal-like arrangement in small domains. Average domain sizes are in the range 10^{-2}–10^{2} μm in diameter.[5,9,10]

Previous studies mainly dealt with the photopolymerization of long-chain fatty acids,[9,11] their cadmium salts,[3-5,9,10] phospholipids,[6-8] and lipid analogues.[12] Polymerization properties of cationic amphiphiles, however, have been studied much less in detail.

Cationic amphiphiles with pyridine and bipyridine units as polar headgroups, for example, are of interest because of their ability to form a variety of salts and metal complexes, acting as carriers able to incorporate photochemically and photophysically active moieties in lipid bilayer-type structures. Corresponding amphiphiles with 4,4'-bipyridine units as polar headgroups are excellently suited as mediators in the photochemically induced generation of hydrogen from water, acting as functional electron relays.[13,14]

Further, *N*-alkylpyridinium salts easily form micellar aggregates in aqueous solution[15] and are adsorbed by inorganic materials.[16] Polymerization of thin layers or bilayer type aggregates of these compounds should stabilize the corresponding structures. A novel type of ultrathin stable devices with potential biophysical applications would thus become accessible.

In a previous study, the polymerization properties of pyridine amphiphiles carrying the hydrophobic tail at the 4-position, e.g., 4-(((*n*-pentacosa-10,12-diynyl)oxy)-carbonyl)pyridine, and some of its salt and metal complex derivatives, have been reported.[17] This study describes the polymerization properties of *N*-alkylpyridinium salts and analogous *N,N'*-dialkyl-4,4'-bipyridinium salts, so-called viologenes, both containing diyne units in their aliphatic chains. Besides the polymerization in the crystalline state, attempts to polymerize these compounds in less ordered systems such as Langmuir–Blodgett multilayers, vesicles, or micelles will be reported.

The amphiphile structures are shown together with abbreviations.

†New address: Ciba-Geigy AG, Forschungszentrum KA, CH-1701 Fribourg, Switzerland.
‡New address: Max-Planck-Institut für Polymerforschung, Jakob-Welder-Weg 11, D-6500 Mainz, West Germany.

0024-9297/85/2218-0327$01.50/0

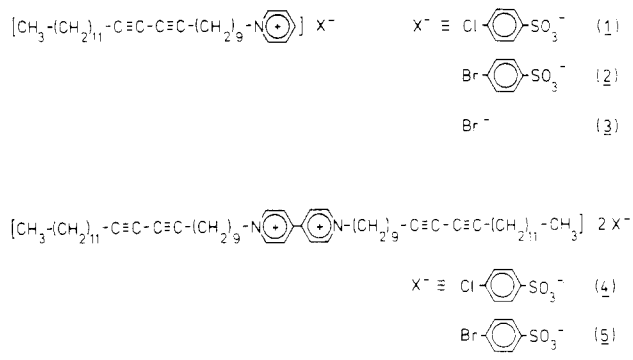

Experimental Section

Preparation of the Amphiphiles. The pyridinium and bipyridinium salts **1–5** were prepared from pyridine or 4,4′-bipyridine by N-alkylation with 1-(((4-chlorophenyl)sulfonyl)oxy)-*n*-pentacosa-10,12-diyne (**7**), 1-(((4-bromophenyl)sulfonyl)oxy)-*n*-pentacosa-10,12-diyne (**8**), or 1-bromo-*n*-pentacosa-10,12-diyne (**9**). Compounds **7–9** were obtained from *n*-pentacosa-10,12-diyn-1-ol (**6**)[10] as the starting reagent.

***N*-(*n*-Pentacosa-10,12-diynyl)pyridinium 4-Chlorobenzenesulfonate (1).** According to the procedures of Sondermann,[18] 15.0 g of 4-chlorobenzenesulfonyl chloride was added to a mixture of 18.0 g of **6** and 8.5 mL of triethylamine in 60 mL of dichloromethane. After stirring for 24 h, the reaction mixture was washed with water and dried over Na_2SO_4, and the solvent was removed in vacuo. The crude 4-chlorobenzenesulfonate ester **7** was recrystallized three times from methanol. Colorless platelets were obtained which turned purple in daylight: yield, 15.2 g (56.3%).

7 (10.7 g, 0.02 mol) thus obtained was allowed to react with 5 mL of pyridine by refluxing the reaction mixture in 280 mL of dry acetonitrile for 24 h. After cooling, the reaction mixture was poured into 2 L of dry ether. The crude pyridinium salt **1** precipitated as a white solid, which was filtered off and recrystallized several times from methanol: colorless platelets; yield, 10.2 g (83.2%); ^{1}H NMR ($CDCl_3$, Me_4Si) δ 0.88 (3 H, t, CH_3), 1.24–1.56 (32 H, br s, CH_2), 1.84 (2 H, s, $>NCH_2CH_2$), 2.28 (4 H, t, $\equiv CCH_2$), 4.80 (2 H, t, $>NCH_2$), 7.33 (2 H, d, anion), 7.80 (2 H, d, anion), 8.08 (2 H, t, py), 8.44 (1 H, t, py), 9.16 (2 H, d, py); IR (KBr) 2940, 2860 (CH, s), 1635 (py, m), 1574, 1500 (ar, m), 1490–1470 (CH_2, s), 1220–1200 (RSO_3^-, v s), 1170–1000 (ar, s), 745 (CH, s) cm^{-1}.

***N*-(*n*-Pentacosa-10,12-diynyl)pyridinium 4-Bromobenzenesulfonate (2).** The 4-bromobenzenesulfonate ester **8** was similarly obtained in 60% yield from **6** and 4-bromobenzenesulfonyl chloride. Colorless platelets were obtained which turned dark red in daylight. Subsequent reaction with pyridine produced the corresponding pyridinium salt **2**: colorless platelets; yield, 10.2 g (89.8%).

***N*-(*n*-Pentacosa-10,12-diynyl)pyridinium Bromide (3).** According to the procedure of Mori,[19] 3 g of phosphorus tribromide in 20 mL of dry ether was added slowly to a solution of 7.2 g (0.02 mol) of **6** in 30 mL of dry ether, while the temperature was kept between 0 and +5 °C. After stirring for 1 h, the reaction mixture was washed with water and dried over Na_2SO_4, and the solvent was removed in vacuo. The crude bromide **9** was recrystallized three times from methanol. A microcrystalline white powder, which rapidly turned greenish blue in daylight, was obtained in a yield of 3.6 g (42.0%). The absorption maximum of the initially formed polymer appears at an usually long wavelength of 685 nm. Subsequent reaction of 3.6 g of **9** with 2.5 mL of pyridine produced the corresponding pyridinium bromide **3**: colorless platelets were obtained which turned purple in daylight; yield, 1.8 g (42%).

***N*,*N*′-Dialkylated 4,4′-Bipyridinium Salts.** The bipyridinium salts **4** and **5** were obtained according to a procedure described in the literature[20] by refluxing 2 mmol of 4,4′-bipyridine and 4 mmol of **7** or **8**, respectively, in 70 mL of dry acetonitrile. *N*,*N*′-bis(*n*-pentacosa-10,12-diynyl)-4,4′-bipyridinium bis(4-chlorobenzenesulfonate) (**4**) was obtained as a microcrystalline powder which rapidly turned blue in daylight; yield, 0.7 g (28%). *N*,*N*′-bis(*n*-pentacosa-10,12-diynyl)-4,4′-bipyridinium bis(4-bromobenzenesulfonate (**5**): microcrystalline powder which rapidly turned orange in daylight; yield, 1.2 g (45%); ^{1}H NMR ($CDCl_3$, Me_4Si) δ 0.92 (6 H, t, CH_3), 1.24–1.56 (64 H, br s, CH_2), 1.88 (4 H, s, $>NCH_2CH_2$), 2.28 (8 H, t, $\equiv CCH_2$), 4.64 (4 H, s, $>NCH_2$), 7.48 (4 H, d, anion), 7.76 (4 H, d, anion), 8.80 (4 H, s, bpy), 9.16 (4 H, s, bpy); IR (KBr) 2940, 2860 (CH, s), 1655 (bpy, s), 1480 (CH_2, s), 1230–1200 (RSO_3^-, vs), 1150–1000 (ar, m), 755 cm^{-1} (CH, m).

Polymerization. The polymerization was carried out either by exposing the crystals to a ^{60}Co γ-ray source, or by UV irradiation of the crystals, multilayers, or dispersions using a 6-W low-pressure mercury lamp (λ = 254 nm). The distance between sample and UV lamp was 10 cm. Care was taken that the temperature never exceeded 25 °C during the polymerization procedure.

Conversion vs. Dose Curves. The polymer content of the crystals was either determined gravimetrically or spectroscopically. For gravimetrical determination residual monomer was extracted from partially polymerized crystals using a solvent which only dissolved the monomer, e.g., hot ethanol. The monomer extraction was repeated until a constant weight was obtained. For a spectroscopic determination the partially polymerized crystals were dissolved in a 1:1 mixture of chloroform and methanol. Subsequently, the optical density of the maximum of the polymer absorption (λ_{max} = 466 nm) was determined, this being a direct function of the polymer content of the crystals.

Optical Spectra. Absorption and diffuse reflectance spectra were monitored by using a Perkin-Elmer Hitachi 200 spectrometer.

X-ray Diffraction Measurements. X-ray diffraction patterns were photographically recorded by using a Kiessig camera. The powderized samples were kept in 0.5-mm glass capillaries, while Ni-filtered Cu Kα radiation was used.

Differential Scanning Calorimetry (DSC). DSC measurements were carried out on a Perkin-Elmer DSC-2 apparatus, using sealed aluminum pans. The heating rate was 20 °C/min.

Monolayer Measurements. The π–A isotherms were studied by using a commercially available Langmuir trough (700 × 150 × 6 mm) equipped with a film balance (MGW Lauda). The monolayers were obtained by spreading solutions of the amphiphiles in chloroform (spectroscopic grade) at a concentration of 1 mg/mL. Triply distilled water was used as the subphase, the third distillation was performed under a nitrogen atmosphere. The resulting pH was 5.8.

Langmuir–Blodgett (LB) Multilayers. The monolayers were transferred onto quartz substrates (size 28 × 12 × 1 mm) by the LB technique. For this purpose the monolayers were compressed to a surface pressure of 30 mN/m at a compression rate of 9 mm/min. The dipping rate was 0.05 mm/s.

Formation of Micelles and Bilayer Aggregates (Vesicles). Aqueous suspensions of the amphiphile **2** (0.5–1.0 mg/mL) formed clear (micellar) solutions at temperatures above 46.5 °C. Upon cooling, a milky white suspension occurred which turned into a translucent, slightly opaque dispersion of bilayer aggregates upon sonication (Bransonic 220, 20 °C, 30 min). Translucent dispersions were also obtained, if clear micellar solutions were sonicated while recooling to room temperature (sonication for 30 min; temperature of sonication bath, 20 °C).

For electron microscopy 1 mL of an aggregate dispersion (0.05–0.2 mg/mL) was mixed with 1 mL of 2% aqueous uranyl acetate and sonicated for 30 min. The dispersion was then applied to a carbon-coated grid and dried in vacuo. A Philips EM 400 electron microscope was used for the measurements.

Results and Discussion

Polymerization in the Crystalline State. *N*-(*n*-Pentacosa-10,12-diynyl)pyridinium Salts. Some of the properties of the pyridinium salts **1–3** and the intermediate products **6–9** are summarized in Table I. It is seen that all the compounds are photoreactive upon UV and γ-irradiation. A thermally initiated polymerization could not be detected for any of the compounds.

Conversion vs. dose curves for the γ-irradiation of the pyridinium salts are shown in Figure 1. The conversion data were determined either gravimetrically by weighing the insoluble polymer formed upon the irradiation process or spectroscopically by monitoring the absorption spectra

Table I
Characteristic Data and Polymerization Properties of the Amphiphiles 1-5 and the Intermediate Products 6-9

compd no.		C, H anal. calcd	C, H anal. found	mp, °C	photoreact upon UV	photoreact upon γ-irradn	polymer absorp λ_{max},[b] nm	polymer soluble?
1	% C:	70.47	70.31	102	+	+	465	+[c]
	% H:	8.48	8.71					
2	% C:	65.65	66.05	115	+	+	465	+[c]
	% H:	7.90	8.14					
3	% C:	71.71	72.17	45	+	+	520	-
	% H:	9.58	9.96					
4	% C:	70.53	70.53	[a]	+	+	620	-
	% H:	8.33	8.11					
5	% C:	65.75	65.22	[a]	+	+	470	-
	% H:	7.76	7.97					
6	% C:	83.26	82.94	56	+	+	600	-
	% H:	12.30	12.31					
7	% C:	69.57	68.97	44	+	+	600	-
	% H:	8.85	8.97					
8	% C:	64.23	63.87	50	+	+	580	-
	% H:	8.17	8.14					
9	% C:	70.92	70.11	38	+	+	685	-
	% H:	10.17	10.33					

[a] See Table III. [b] At low conversion to polymer (<0.1%). [c] In chloroform/methanol 1:1.

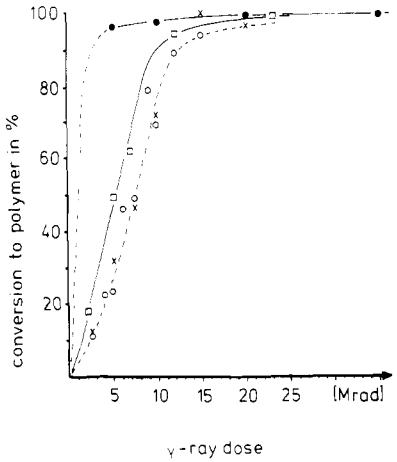

Figure 1. Plot of fractional polymer conversion vs. ^{60}Co γ-ray dose for compounds **1** (□), **2** (○, ×), and **3** (●). Conversion data of **2** have been determined gravimetrically (○) and spectroscopically (×).

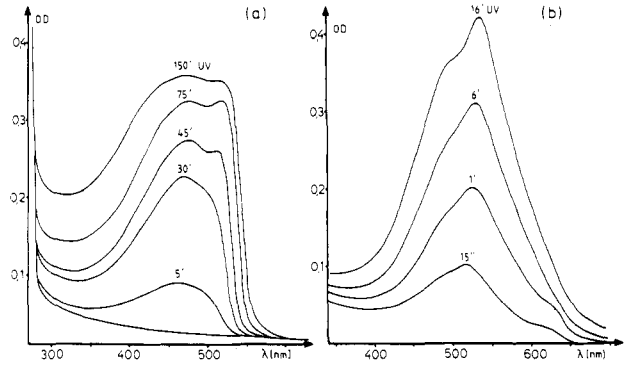

Figure 2. Absorption spectra of solution cast films of **1** (a) and **3** (b) as a function of the UV-irradiation time.

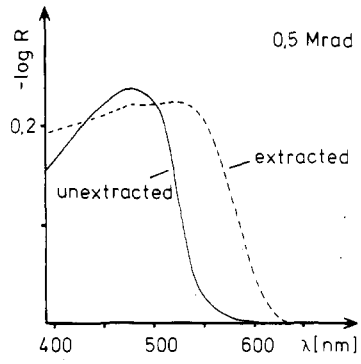

Figure 3. Diffuse reflectance spectra of **1** exposed to a γ-ray dose of 0.5 Mrd and after extraction of residual monomer with ethanol.

of the polymer in solution, as it will be discussed in more detail below. All compounds are converted into polymers nearly completely. For compounds **1** and **2** a marked increase in reaction rate can be detected, once a conversion to polymer of about 20% is exceeded.

Although the three compounds only vary in the nature of their counterions, their reaction kinetics are considerably different. This is due to a crystal lattice control of the polymerization process, the anions controlling the packing geometries of the photoreactive *N*-alkylpyridinium cations. The polymerization can also be followed by absorption spectroscopy due to the conjugated structure of the backbone -[C≡C—C(R)=(R′)]-, strongly absorbing in the visible (R and R′ are the substituent groups $C_{12}H_{25}$ and $(CH_2)_9NC_5H_5^+X^-$, respectively).

Absorption spectra of solution cast films of the compounds **1** and **3** monitored after different UV irradiation times are shown in Figure 2. The films consist of thin transparent microcrystals of the amphiphiles. Their thickness is ≤1 μm. Figure 2 indicates an increase in the absorbance due to polymer formation as a function of the UV-irradiation time. **3** exhibits a higher photoreactivity than **1**, as the fast increase in the polymer absorbance shows. The band shapes of the absorption spectra of the two polymerized amphiphiles differ considerably and are a function of the UV-irradiation time. It should be added that the absorbance of **2** is identical with that of **1**, both showing a maximum absorption at a wavelength of 470 nm initially, which shifts to 540 nm at higher conversions to polymer. The yellow-to-red color change of the crystals occurs at about 20% conversion to polymer and is accompanied by an increase of the polymerization rate. The same color change occurs, if residual monomer is leached out of the partially polymerized yellow crystals, as shown by the diffuse reflectance spectra of Figure 3.

This color change had also been observed for other diacetylene derivatives[21] and was attributed to a change of the backbone conformation from an initially distorted nonplanar to a planar structure, simultaneously increasing

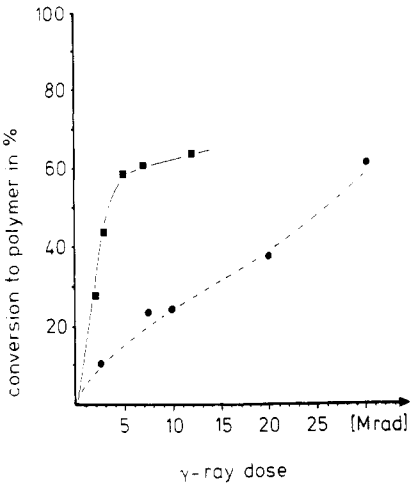

Figure 4. Plot of fractional polymer conversion vs. ^{60}Co γ-ray dose for compounds **4** (■) and **5** (●).

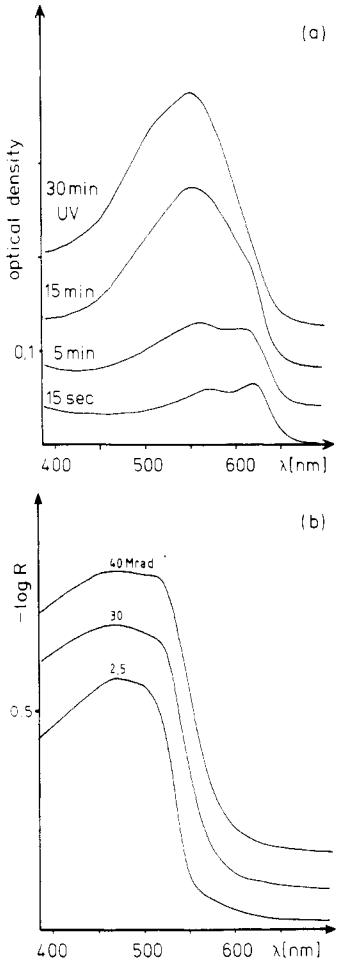

Figure 5. Absorption spectra of a solution cast film of **4** as a function of the UV-irradiation time (a), and diffuse reflectance spectra of **5** after various γ-ray doses (b).

the effective conjugation length.[21]

In a similar way, partially polymerized crystals of **3**, which initially exhibit a purple color, turn red, if residual monomer is leached out. Again monomer extraction from the crystal lattice causes a conformational transition of the backbone, in which the thermodynamically more stable "red" modification is formed.[11]

***N,N'*-Bis(*n*-pentacosa-10,12-diynyl)-4,4'-bipyridinium Salts.** Some of the properties of the bipyridinium salts **4** and **5** are listed in Table I. Both the amphiphiles are reactive upon UV and γ-irradiation, whereas a thermally initiated polymerization is not observed.

Table II
Layer Spacings of the Monomeric and Polymeric Amphiphiles as Determined by X-ray Scattering

compd no.	layer spacing d_{001}, nm monomer	polymer[a]
1	4.22	4.09
2	4.26	4.11
3	3.62	3.56
4	4.55	4.49
5	4.03	3.94

[a] Crystals exposed to γ-ray dose of 10 Mrd.

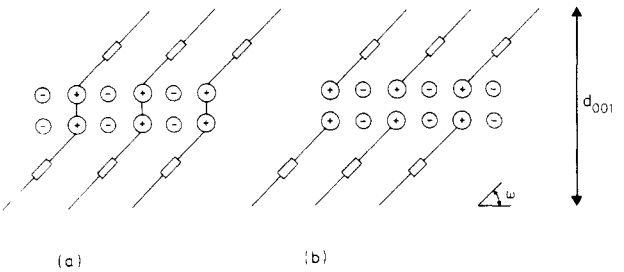

Figure 6. Schematic illustration of the bilayer structure of the amphiphiles **4** and **5** (a) and **1**–**3** (b) in the crystalline state: straight line, hydrocarbon chain; rectangle, diyne unit; circle (+), pyridinium (bipyridinium) cation; circle (–), counterion.

Conversion vs. dose curves determined for γ-irradiation in the crystalline state are shown in Figure 4. Both compounds are converted into polymers only partially. **4** exhibits a rapid polymerization initially, which ceases at a conversion to polymer of about 60%. **5** is only slightly photoreactive.

Figure 5 shows the absorption spectra of a solution cast film of **4**, exposed to UV light for different irradiation times (film thickness ≤1 μm). Since **5** could not be obtained as a transparent film, the spectra of **4** were compared with diffuse reflectance spectra of microcrystalline powders of **5**, exposed to various γ-ray doses. As the spectra indicate, **4** forms a blue polymer initially, turning purple at higher irradiation doses, whereas spectra of **5** resemble those of **1** and **2**.

As already discussed for the pyridinium salts, the different polymerization properties of **4** and **5** are most likely a consequence of variations of the packing geometries of the monomers. Incomplete conversion of **4** may originate from a phase transition to a less reactive modification, induced by the polymerization process. A similar behavior has been observed for long-chain diacetylene fatty acids.[11]

However, the photoreactivity of monomers containing two or more reactive units per molecule may also be diminished for another reason. Since polymerization of the diyne units controls the arrangement of the side groups in the crystal lattice,[22,23] the reaction of one of the units will affect the packing geometry of the other unit and possibly render its reaction more difficult. Low photoreactivities were found for a number of bifunctional diacetylene derivatives, such as 4,4'-bis(((*n*-pentacosa-10,12-diynyl)oxy)carbonyl)-2,2'-bipyridine, for example.[17]

Structural Aspects. Structural studies of microcrystalline powders of the amphiphiles were carried out by X-ray scattering methods. In Table II the layer spacings of the monomers and polymers are listed, as determined from Debye and Kiessig powder patterns.

Due to their amphiphilic character it seems most likely to us that the various compounds crystallize in a head-

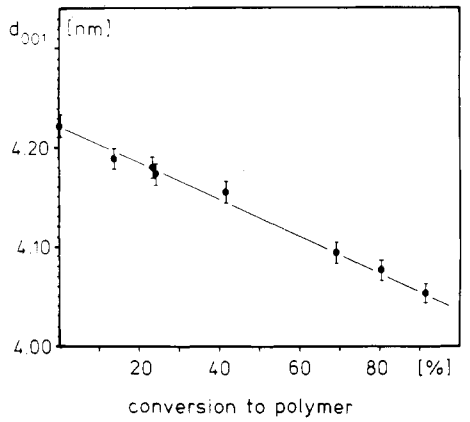

Figure 7. Plot of the layer spacing d_{001} of **1** as a function of the fractional conversion to polymer.

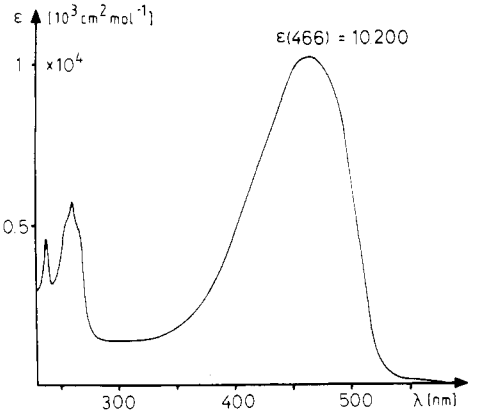

Figure 8. Absorption spectrum ofthe polymer of **1** dissolved in a 1:1 mixture of chloroform and methanol.

Table III
Melting Behavior of the Bipyridinium Salts 4 and 5 (as Monomers)

	phase transitions, °C			
compd no.	solid–solid	solid–LC	LC–LC	decomp, °C
4	54	107		250
5	67	111	190	270

to-head (bilayer type) fashion, as it is schematically shown in Figure 6. However, it must be admitted that also a head-to-tail structure cannot be ruled out from the structural data available at present. Assuming the bilayer-type arrangement, the counterions of compounds **4** and **5** will be arranged in positions near to the bipyridinium dications and thus keep the distances between the dications large (Figure 6a). Consequently, a dense packing of the paraffin chains can only occur, if the tilting angle ω of the chain axes with respect to the layer plane is low. This is in fact true, as the low values of the layer spacings listed in Table II indicate. The chain axes must be strongly tilted, because the d_{001} values of **4** and **5** of 4.55 and 4.03 nm, respectively, are much shorter than the molecular lengths of about 7.50 nm, deduced from molecular models.

Assuming that the innermost reflection occurring in the X-ray diffraction diagrams can be indexed as (001) reflection, compounds **1–3** likely exhibit packing geometries similar to those of **4** and **5** (Figure 6b). However, it must be admitted that the innermost reflection can also be indexed as (002), which would indicate an almost perpendicular orientation of the paraffin chains with regard to the layer plane.

1 and **2** are likely isomorphic, as the small differences of the layer spacings of 0.04 nm as well as the similar polymerization properties indicate. For these reasons the structures of **1** and **2** will also be similar to that of **5**. **3** (and **4**) fall out of the series and exhibit smaller (or larger) tilting angles ω of the paraffin chain axes with regard to the layer plane.

During polymerization the layer spacing of the compounds is decreasing (Table II). The decrease is almost a linear function of the conversion to polymer, as observed for **1** in Figure 7. This points to a homogeneous reaction. A discontinuous phase transition of the aliphatic side groups, as observed for long chain diacetylene fatty acids in multilayers,[24] for example, does not occur.

Thermal Properties. The pyridinium salts **1–3** form isotropic melts and do not exhibit phase transitions between −30 °C and the melting points (see Table I), whereas the bipyridinium salts **4** and **5** undergo several reversible transitions until decomposition occurs at temperatures above 250 and 270 °C, respectively. The phase transition temperatures are listed in Table III. The transitions below 100 °C are solid-to-solid transitions, while the other ones result in the formation of liquid crystalline phases, as seen from their behavior in polarized light. Polymerization causes the complete disappearance of the phase transitions. Simultaneously the decomposition temperatures increase to values of about 300 °C.

Polymeric crystals of **4** exhibit thermochromic properties. In the temperature range between 54 and 107 °C the color gradually and reversibly changes from blue or deep purple, depending on the polymer content, to red and finally orange. Heating to temperatures above 107 °C causes an irreversible color change to red. At this temperature the residual monomer undergoes a solid-to-liquid crystalline transition. This causes a phase separation of monomer and polymer, allowing the polymer to relax to the more stable red structure irreversibly. In the liquid crystalline state the monomers are photoinactive if irradiated with UV light.

Solution Properties of the Polymers. The polymeric pyridinium salts **1** and **2** are soluble in a 1:1 mixture of chloroform and methanol and insoluble in all other common organic solvents. The amphiphiles **3–5** are completely insoluble, even in the chloroform/methanol solvent mixture.

The polymer solutions exhibit a yellow color with an absorption maximum at 466 nm and a molar absorptivity ϵ_{466} of 10 200 L·mol^{-1}·cm^{-1}, arising from the conjugated backbone (Figure 8). Additional absorption maxima of the pyridine moiety and the 4-chloro- or 4-bromobenzenesulfonate counterions occur at 260 and 240 nm.

The solubility can be utilized for a spectroscopic determination of the amount of polymer formed in the crystals.[17,25] Conversion data of γ-irradiated crystals of **1** obtained spectroscopically and gravimetrically are in good agreement, as indicated by Figure 1.

Addition of electrolytes (NaBr, LiCl) to a polymer solution in chloroform/methanol causes the rapid precipitation of the polymer as a red solid. Probably the polymeric halide salts are formed, which are completely insoluble, as the example of the polymeric compound **3** indicates. This experiment demonstrates a strong influence of the counterions on the solubility of the polymer.

Polymerization in LB Multilayers. Stability of Monomolecular Layers. Spreading of the amphiphiles at the air–water interface results in the formation of monomolecular films, which are characterized by their π–A isotherms, as shown in Figure 9. All compounds form liquid-expanded films on a subphase of pure water even at temperatures below 5 °C. However, the counterion strongly influences the monolayer properties. While the

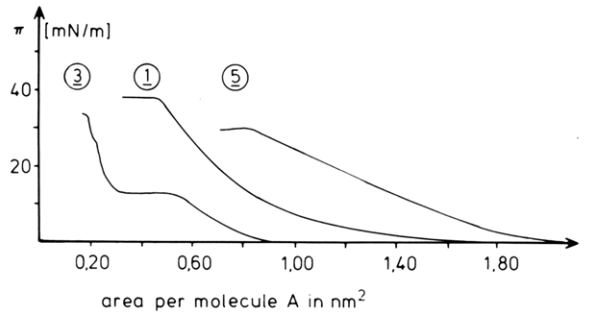

Figure 9. π–A isotherm of monomolecular layers of **1**, **3**, and **5** (T = 15 °C, subphase: pure water, pH 5.8).

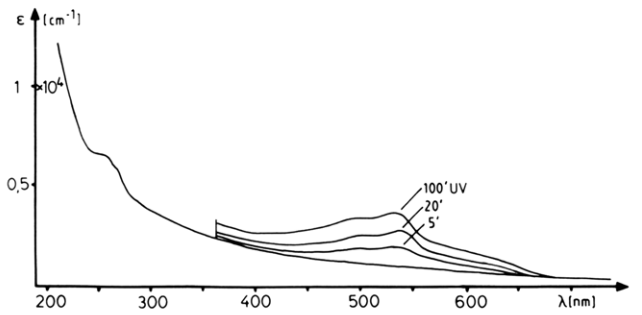

Figure 10. Polymerization in LB multilayers built up on a quartz substrate. Absorption spectra of 28 layers of a mixture of **3** and cadmium arachidate in a molar ratio of 1:2.8 as a function of the UV-irradiation time.

monolayer is compressed, the chlorobenzenesulfonate salt **1** only forms a liquid film, whereas the bromide salt **3** exhibits a transition from the liquid-expanded to the condensed state. Presence of sodium bromide in the subphase in a concentration of 10^{-3} mol/L has no effect on the π–A isotherm of **1**. This allows the conclusion that there is no exchange of the chlorobenzenesulfonate ions by the excess bromide ions at the interface. Instead the chlorobenzenesulfonate ions are likely incorporated in the monomolecular film and thus reduce the packing density of the amphiphilic cations.

An additional reason for the low film stabilities could be an orientation of the pyridine (bipyridine) head groups and the counterions parallel to the water surface. A flat position would allow a maximum interaction of the polar nitrogen atom of the pyridine ring with the water subphase, and the large area occupied would also prevent a dense packing of the aliphatic chains.

Photoreactivity in Multilayers. The polymerization of monolayers of the diacetylene amphiphiles can be monitored directly by UV/Vis absorption spectroscopy, if the monolayers are deposited on quartz substrates by the LB technique.[14,24] However, due to their low film stabilities the pyridinium and bipyridinium salts could only be deposted as mixed monolayers "diluted" with cadmium arachidate. In Figure 10 the absorption spectra of a multilayer are shown consisting of 28 layers of **3** and cadmium arachidate in a molar ratio of 1:2.8. The formation of polymer is indicated by the optical absorption with a maximum at about 540 nm, which builds up as a function of the UV-irradiation time.

Polymerization in Aqueous Dispersion. Aqueous suspensions of the *N*-alkylpyridinium salts **1**–**3** turn into clear, micellar solutions at elevated temperatures. The micelle formation sets in above a critical concentration (cmc) of 0.00122 mol/L (T = 46.5 °C). At temperatures below 46.5 °C the micellar solutions turn into milky white suspensions, from which the amphiphiles precipitate within a few hours. Sonication of the freshly prepared suspensions for 30 min results in the formation of translucent, slightly opaque dispersions of spherical aggregates.[26,27]

Electron micrographs of the aggregates negatively stained with uranyl acetate (1% by weight) are shown in Figure 11. Directly after sonication spherical particles of diameters between 100 and 250 nm are formed (Figure 11a), which likely represent vesicles, though a finite proof, for example by entrapment of an aqueous marker, is still lacking. Within a few hours the spherical aggregates re-

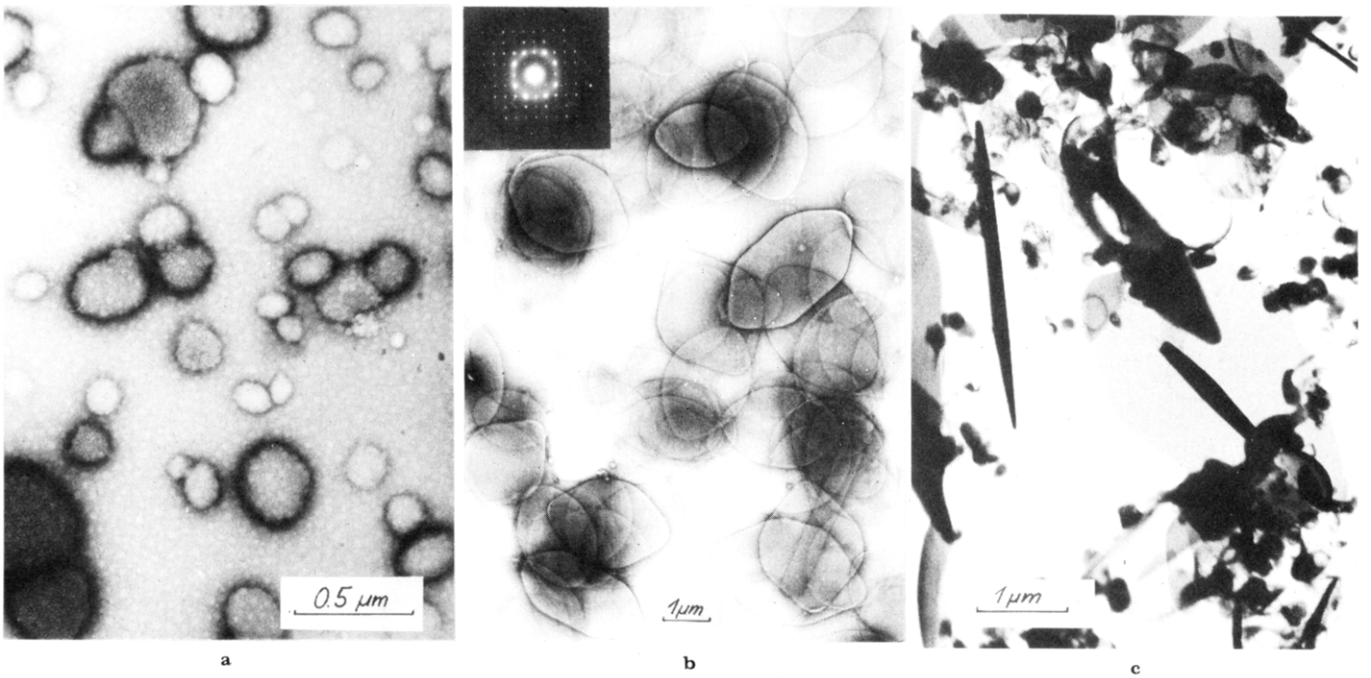

Figure 11. Electron micrographs of monomeric aggregates of **2**, directly after sonication of the aqueous dispersion (a), and 6 h later (b, c). The inset of (b) shows an electron diffraction pattern of an individual aggregate. (c) shows aggregates in different orientations, which were obtained upon gradual heating of a frozen dispersion inside the electron microscope. Sample solutions 0.05 mg/mL, negatively stained (a, b) with 1% uranyl acetate (by weight).

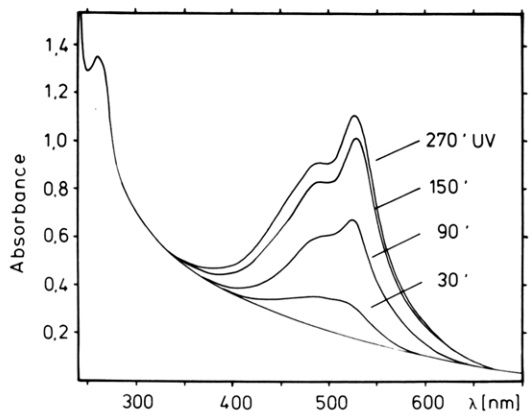

Figure 12. Absorption spectra of an aggregate dispersion of **2** (concentration 0.07 mg/mL) in a 1-cm cuvette before exposure to a 6-W low-pressure mercury lamp (lower curve) and after various exposure times.

arrange into multilamellar layers with average diameters of a few micrometers (Figure 11b,c). Dispersions of these aggregates are stable for 3–4 days until precipitation sets in.

The individual aggregates of oval or polygonal shape are very thin. This is visualized in Figure 11c, where some of the platelets are seen edge on. The random orientation occurs when a dispersion is frozen on a copper grid to liquid nitrogen temperature and gradually heated inside the electron microscope to sublime the solvent.

Electron diffraction patterns of the vesicles exhibit a diffuse halo. In contrast to this behavior, the larger aggregates give rise to crystalline reflections which can be used to determine the unit cell.[28] An example of the diffraction patterns is inserted in Figure 11b.

The photoreactivity of **2** in aqueous dispersions was studied by exposing a micellar solution as well as a freshly sonicated aggregate dispersion to UV light for different time periods. Micellar solutions remained completely unchanged, even after irradiation for several hours. Aggregate dispersions turned orange and finally red, indicating a photopolymerization of the diyne units. Absorption spectra of an aggregate dispersion of **2** monitored after different UV-irradiation times are shown in Figure 12.

Electron micrographs of polymerized dispersions only show aggregates of diameters larger than a micrometer (Figure 13a,b). Presumably the initially present spherical particles of diameters of about 100 nm (Figure 11a) were photoinactive and rearranged into larger aggregates which subsequently polymerized.

Most of the aggregates exhibit a polygonal rather than an oval shape, which may be a consequence of the polymerization process. Features like the "tails" occurring in many of the aggregates have also been observed for polymerized liposomes of double-chain diacetylene amphiphiles.[31] Its origin is unclear. Electron diffraction patterns of individual polymerized aggregates indicate a unqiue orientation of the molecules (Figure 13a). However, from the few spots seen in the diffraction pattern it can be concluded that the molecules are less ordered than in the corresponding monomeric aggregates.

The polymerized dispersions are stable in the dark for several weeks. Heating neither causes a transition into micellar aggregates nor does it cause a precipitation of the polymer. However, heating is accompanied by a color change from red to orange, as shown in Figure 14 and similarly observed upon a dissolution of the polymer. The color change is only partially reversible and may arise from

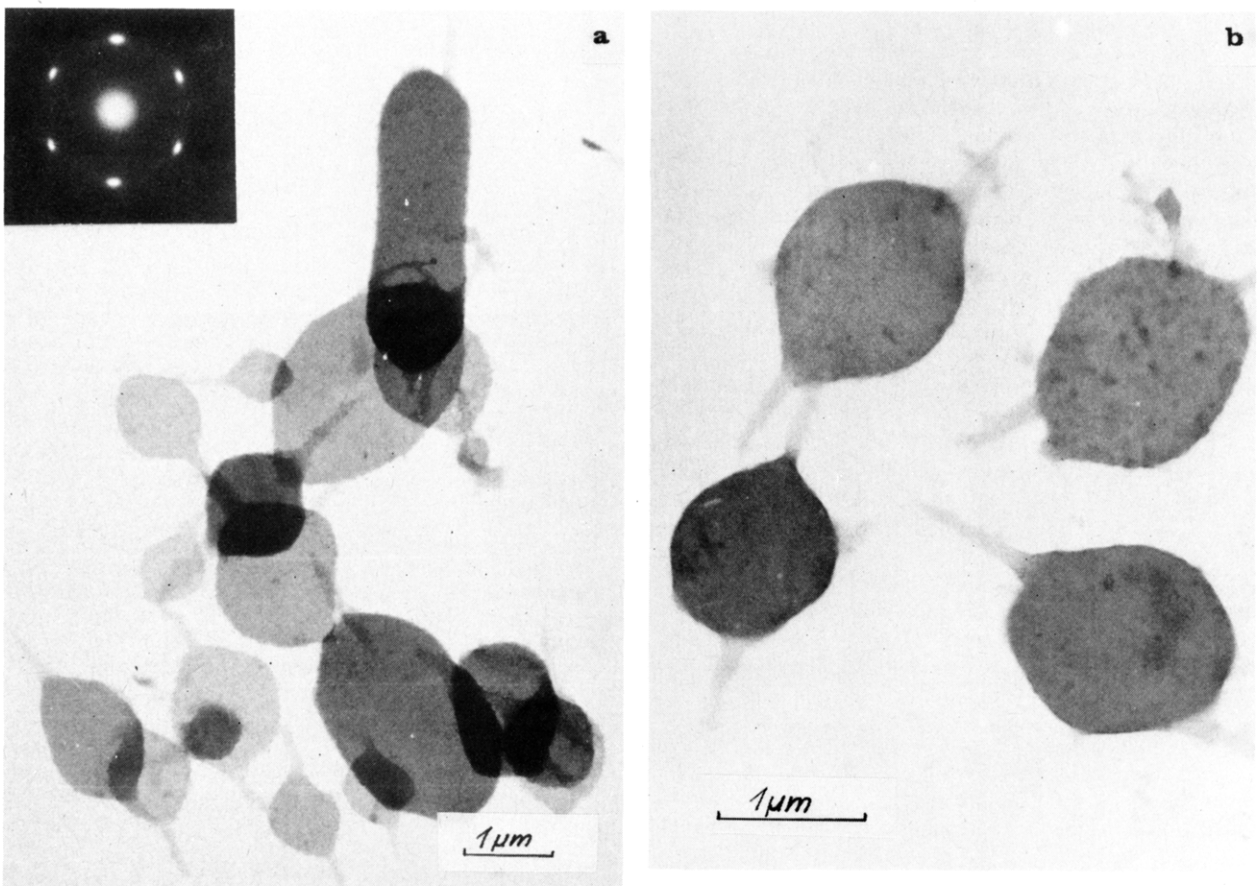

Figure 13. Electron micrographs of polymerized aggregates of **2**. Aggregates UV irradiated for 5 h. Sample solution 0.05 mg/mL. The inset of (a) shows an electron diffraction pattern of an individual aggregate.

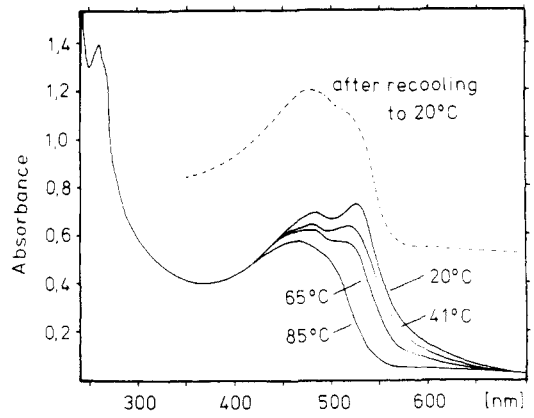

Figure 14. Absorption spectra of a polymerized dispersion of **2** at different temperatures, and after recooling to 20 °C (---). Sample in a 1-cm cuvette, 24 h after UV irradiation (concentration 0.05 mg/mL).

a conformational transition of the conjugated backbone,[29,30] due to an increased molecular mobility at elevated temperatures.

Polymerized dispersions decolorize upon exposure to daylight within a few days, indicating a decomposition of the conjugated backbone. Possibly the N-alkylated pyridinium moieties are photochemically reduced by the water molecules under simultaneous formation of OH· radicals. OH· radicals are known to decompose the polydiacetylene backbone rapidly.[30]

Concluding Remarks

The N-alkylated pyridinium salts **1–3** can be polymerized completely in a crystal lattice controlled reaction without phase transitions of the aliphatic side groups. This is in contrast to the other amphiphilic diacetylene derivatives, which can only partially be converted into polymer in yields up to approximately 60–80%.[11,17]

The pyridinium and bipyridinium salts are less suited for a polymerization in monomolecular layers or LB multilayers. Spherical aggregates (vesicles) of the pyridinium salts are very unstable and rearrange into multilamellar layers of high crystallinity. A high surface curvature possibly renders the topochemical polymerization difficult in vesicles, allowing the rearrangement to occur much faster than the polymerization of the vesicles. Lopez et al. already reported that small vesicles of lipid diacetylenes were less sensitive to light than larger ones.[12b] After rearrangement the aggregates are highly photoreactive. Since the polymerization preserves the aggregates from precipitation, highly stable aqueous dispersions become accessible, which can be utilized as stable carriers in a variety of physicochemical and biological applications.[32-34]

The sensitivity of the diyne polymerization to the structural order of the lipid chains can be used to deduce information on the physical state of order of the aggregates. As is indicated by their polymerization in multilayers, the molecules are present in a crystal-like arrangement. In small vesicles (≤100 nm) the lipid chains are less ordered, probably due to the increased surface curvature. The same is true for micelles, where the molecules are likely to be present in a liquid analogous state.[35,36]

Acknowledgment. We thank Monika Stiefvater for valuable technical assistance in the preparation of the amphiphiles and the spectroscopic studies. This work was supported financially by Ciba Geigy AG, Basel, and the Fonds der Chemischen Industrie.

References and Notes

(1) Wegner, G. *Z. Naturforsch., B* **1969**, *24B*, 284.
(2) For a recent review, see: Bloor, D. In "Developments in Crystalline Polymers"; Bassett, D. C., Ed.; Applied Science Publishers, Ltd.: London, 1982.
(3) Tieke, B.; Wegner, G.; Naegele, D.; Ringsdorf, H. *Angew. Chem., Int. Ed. Engl.* **1976**, *15*, 764.
(4) Day, D.; Ringsdorf, H. *J. Polym. Sci., Polym. Lett. Ed.* **1978**, *16*, 205.
(5) Tieke, B.; Lieser, G.; Wegner, G. *J. Polym. Sci., Polym. Chem. Ed.* **1979**, *17*, 1631.
(6) Hub, H.; Hupfer, D.; Koch, H.; Ringsdorf, H. *Angew. Chem., Int. Ed. Engl.* **1980**, *19*, 938.
(7) Johnston, D. S.; Sanghera, S.; Pons, M.; Chapman, D. *Biochim. Biophys. Acta* **1980**, *602*, 57.
(8) O'Brien, D. F.; Whitesides, T. H.; Klingbiel, R. T. *J. Polym. Sci., Polym. Lett. Ed.* **1981**, *19*, 95.
(9) Tieke, B.; Lieser, G.; Weiss, K. *Thin Solid Films* **1983**, *99*, 95.
(10) Tieke, B.; Weiss, K. *J. Colloid Interface Sci.* **1984**, *101*, 129.
(11) Tieke, G.; Bloor, D.; Young, R. J. *J. Mater. Sci.* **1982**, *17*, 1156.
(12) (a) Day, D.; Hub, H.; Ringsdorf, H. *Isr. J. Chem.* **1979**, *18*, 325. (b) Lopez, E.; O'Brien, D. F.; Whitesides, T. H. *J. Am. Chem. Soc.* **1982**, *104*, 305.
(13) Kiwi, J.; Grätzel, M. *Nature (London)* **1979**, *281*, 657; *J. Am. Chem. Soc.* **1979**, *101*, 7214.
(14) Möbius, D. *Acc. Chem. Res.* **1981**, *14*, 63. Seefeld, K. P.; Möbius, D.; Kuhn, H. *Helv. Chim. Acta* **1977**, *60*, 2608.
(15) Anacker, E. W.; Ghose, H. M. *J. Am. Chem. Soc.* **1969**, *91*, 6579.
(16) Lagaly, G.; Stange, H.; Weiss, A. *Kolloid Z. Z. Polym.* **1972**, *250*, 675.
(17) Tieke, B.; Weiss, K. *Colloid Polym. Sci.*, in press.
(18) Sondermann, J. *Liebigs Ann. Chem.* **1971**, *749*, 183.
(19) Mori, K. *Tetrahedron* **1974**, *30*, 3807.
(20) Sprintschnik, G.; Sprintschnik, H. W.; Kirsch, P. P.; Whitten, D. G. *J. Am. Chem. Soc.* **1977**, *99*, 4947.
(21) Patel, G. N.; Duesler, E. N.; Curtin, D. Y.; Paul, I. C. *J. Am. Chem. Soc.* **1980**, *102*, 461.
(22) Enkelmann, V.; Wegner, G. *Angew. Chem.* **1977**, *89*, 432.
(23) Siegel, D.; Sixl, H.; Enkelmann, V.; Wenz, G. *Chem. Phys.* **1982**, *72*, 201.
(24) Tieke, B.; Lieser, G. *J. Colloid Interface Sci.* **1982**, *88*, 471.
(25) Patel, G. N.; Khanna, Y. P.; Yvory, D. M.; Sowa, J. M.; Chance, R. R. *J. Polym. Sci., Polym. Phys. Ed.* **1979**, *17*, 899.
(26) Fendler, J. H. *Acc. Chem. Res.* **1980**, *13*, 7.
(27) Kunitake, T. *J. Macromol. Sci., Chem.* **1979**, *A13*, 587.
(28) Lieser, G.; Tieke, B., unpublished.
(29) Chance, R. R.; Patel, G. N.; Witt, J. D. *J. Chem. Phys.* **1979**, *71*, 206.
(30) Müller, M. A.; Wegner, G. *Makromol. Chem.* **1984**, *185*, 1727.
(31) Wagner, N.; Dose, K.; Koch, H.; Ringsdorf, H. *FEBS Lett.* **1981**, *132*, 313.
(32) Tundo, P.; Kippenberger, D. J.; Politi, M. J.; Klahn, P.; Fendler, J. H. *J. Am. Chem. Soc.* **1982**, *104*, 5352.
(33) Kunitake, T.; Sakamoto, T. *J. Am. Chem. Soc.* **1978**, *100*, 4615.
(34) Gros, L.; Ringsdorf, H.; Schupp, H. *Angew. Chem., Int. Ed. Engl.* **1981**, *20*, 305.
(35) Menger, F. M. *Acc. Chem. Res.* **1979**, *12*, 111.
(36) Fromherz, P. *Ber. Bunsenges. Phys. Chem.* **1981**, *85*, 891.